

PARAMAGNETIC CENTERS IN AMORPHOUS AND MICROCRYSTALLINE SILICON IRRADIATED WITH 2 MeV ELECTRONS

*A. Astakhov^{1,2}, F. Finger², R. Carius², A. Lambertz², I. Neklyudov¹, Yu. Petrusenko¹,
V. Borysenko¹, D. Barankov¹*

¹*National Science Center "Kharkov Institute of Physics & Technology",
Institute of Material Science & Technology, 1, Akademicheskaya st.,
61108, Kharkov, Ukraine;*

²*Forschungszentrum Jülich, Institute of Photovoltaics, 52425 Jülich, Germany*

Amorphous and microcrystalline silicon are well known materials for thin film large area electronics. The defects in the material are an important issue for the device quality and the manufacturing process optimization. We study defects in thin film silicon with electron spin resonance (ESR). In order to vary the defect density in a wide range 2 MeV electron bombardment at 100 K was applied with dose as high as 10^{18} e^{*}cm⁻². Samples were investigated after deposition, after irradiation and between the annealing steps. The spin density (N_s) in the material was varied over 3 orders of magnitude. Strong satellites with $g \approx 2.010$ and $g \approx 2.000$ were observed on the shoulders of the dangling bond line. The initial N_s and the shape of the resonance line were restored after annealing.

INTRODUCTION

Amorphous hydrogenated silicon (a-Si:H) is a widely used material for production of large area electronics, TFTs and photovoltaics [1]. Microcrystalline hydrogenated silicon (μ c-Si:H) is a new promising material for this area of applications, providing high carrier mobility and effective doping. Low substrate temperature during deposition (200...300 °C) together with possibility of large area depositions make these materials attractive for commercial thin films electronics. Great progress has been made in the last decades in understanding of the properties of the silicon based disordered semiconductors [2, 3]. Nevertheless many questions still have to be answered in order to improve nowadays technologies. In particular, clear understanding of the role of defects in the electronic properties of a-Si:H and μ c-Si:H is crucial. The *Electron Spin Resonance* (ESR) technique was long ago found to be a suitable tool for investigation of defects in thin film silicon [2, 3]. ESR being sensitive to the nearest neighborhood of the electron in paramagnetic state could give valuable information on the nature and configuration of the given defect [4]. Unfortunately natural disorder in the investigated material smears out fine structure of the spectrum [2, 3]. Slightly asymmetric ESR lines at g -values in the range of 2.0045...2.0055 with the width of 6-8 gauss characterize the intrinsic thin film silicon [2, 3, 5, 6, 7, 8]. The resonance is commonly assigned to the silicon dangling bonds (db) in different environments [5], but a more accurate identification of the defects in the material is still missing. Defect density management with the post-preparation treatment is required to gain more information on the defect structure. Low temperature bombardment with high-energy electrons was shown to be suitable tool for the reversible enhancement of the defect density in the hydrogenated silicon samples with a microstructure ranging from microcrystalline to amor-

phous [9]. In the report we present results on a-Si:H and μ c-Si:H material where the defect density is varied by electron irradiation and subsequent annealing.

EXPERIMENT SAMPLE PREPARATION

Samples were prepared using *Very High Frequency Plasma Enhanced Chemical Vapour Deposition* (VHF-PECVD) (95 MHz) from silane-hydrogen mixtures. The deposition parameters were constant for all samples in the series: gas pressure 300 Torr, discharge power 0.1 W/cm², and substrate temperature 200 °C. Only the silane to hydrogen ratio ($SC = [SiH_4]/[SiH_4]+[H_2]$) was varied in the gas mixture from run to run in a range of 3...100% leading to structure variation from highly crystalline to completely amorphous. Several samples were deposited with a supplement of PH₃ in the deposition gas mixture in order to achieve n-type doping as high as 5...13 ppm.

The crystalline volume fraction (I_{CRS}) was semi-quantitatively determined from Raman measurements as a ratio between intensities of the Raman signals at 520 cm⁻¹ and 500 cm⁻¹ (attributed to the crystalline phase) and the Raman signal at 480 cm⁻¹ (attributed to the disordered phase), i.e. $I_{CRS} = (I_{500} + I_{520})/(I_{480} + I_{500} + I_{520})$ [10].

Films with 4...7 μ m thickness were deposited on the Mo substrate. The substrate was bent after deposition and peeled off flakes of the deposited films were collected and sealed in quartz tubes at 0.5 bar He atmosphere for ESR measurements.

The ESR was measured in X-band ($F \approx 9.3$ GHz) at temperature of 40 K using lock-in detection technique. The samples preparation and ESR measurements were carried out in the Institute of Photovoltaics (Forschungszentrum Jülich, Germany).

IRRADIATION

The electron bombardment was carried out using the ELIAS Van de Graaf electron accelerator in National Science Center “Kharkov Institute of Physics & Technology” (Ukraine) with energy of 2 MeV and beam current density of $5\mu\text{A}\cdot\text{cm}^{-2}$. A dose of $10^{18}\text{ e}\cdot\text{cm}^{-2}$ was applied for all samples in the present experiment. The irradiation was carried out at a temperature of around 100K in order to reduce self-annealing and exclude the heat damage to the sample. During irradiation samples were cooled with the flow of high-purity N_2 .

Note, that after irradiation samples were transported to the Institute of Photovoltaics (Germany). Therefore to exclude room temperature annealing, samples were stored in the LN_2 -cooled dry transport cryostat. Hence the room temperature exposure was minimized to 2...5 minutes. After the measurements of the irradiated samples an annealing procedure was applied in a step-wise manner with the following sequence: 50, 80, 120, 160 °C, each step was 30 minutes long. The maximum annealing temperature was chosen well below the deposition temperature ($T_s=200\text{ °C}$) in order to avoid changes of the microstructure of the samples.

RESULTS

We investigated ESR of the intrinsic thin film silicon with different structural composition extensively before the electron irradiation experiment [6, 11, 12, 13]. Fig. 1 shows the dependence of the N_s and g -value on the SC during sample preparation.

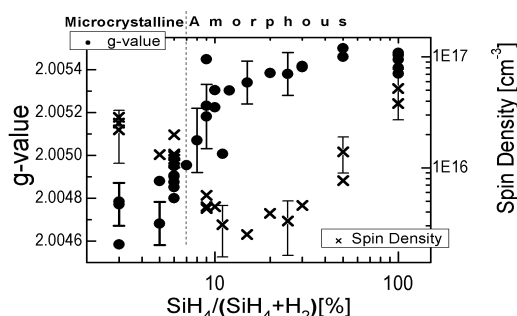


Fig. 1. g -value and the spin density of the samples prepared at various SC. Dashed line approximately indicates the transition from microcrystalline to amorphous structure according to the Raman data

The transition from the microcrystalline to amorphous growth at our deposition conditions is found at $\text{SC}\approx 7\%$ according to the Raman data i.e. samples with $\text{SC}>7\%$ do not show a crystalline peak in the Raman spectra (Raman amorphous). There is a clear systematic shift of the g -value between microcrystalline and amorphous material. The g -value increases in the vicinity of transition (with increase of the amorphous phase fraction) from $g\approx 2.0047$ to $g\approx 2.0050$. Note, that the g -value increases further beyond the transition to amorphous structure ($\text{SC}=8\text{...}15\%$). The saturation was found only at $\text{SC}>50\%$ at $g\approx 2.0054$. The g -value shift is expected due to the difference of the dangling bond environment in $\mu\text{c-Si:H}$ and a-Si:H .

The shift of the g -value after transition to amorphous growth, where no crystalline peak could be seen in the Raman spectra, however is surprising. The region is interesting because the N_s has a minimum here and the material prepared within the region is known to be the best absorber layer for the amorphous thin film silicon solar cells.

The Fig. 2,a shows the ESR spectra before and after irradiation. Note that all spectra are normalized to the same peak-to-peak height for the lineshape comparison. Fig. 2,b is a plot of the spin density vs. silane concentration before and after irradiation. The spin density after irradiation increases by 3 orders of magnitude and qualitatively repeats the N_s vs. SC dependence before irradiation. No significant shift of the resonance line from the initial position of the db line was detected after irradiation, but significant change of the lines shape is clearly seen (Fig. 2,a). Remarkable additional features appear on the shoulders of the central db line at g -values around 2.000 and 2.010. These features were found in the spectra of all irradiated samples having different configuration for different material structures.

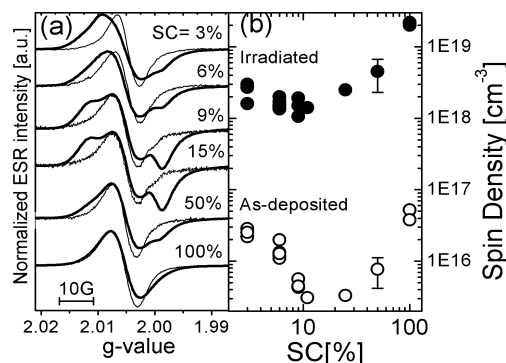


Fig. 2. ESR spectra of a-Si:H and $\mu\text{c-Si:H}$ with different silane concentration before (thin) and after (bold) irradiation (a); Spin density of the material prepared with different SC before and after irradiation (b)

After irradiation annealing was applied to the samples. In Fig. 3,a spin densities of the intrinsic samples after annealing steps are presented. The N_s of the db line was increased after irradiation as was mentioned above. During annealing all samples show return of the N_s close to as-deposited value.

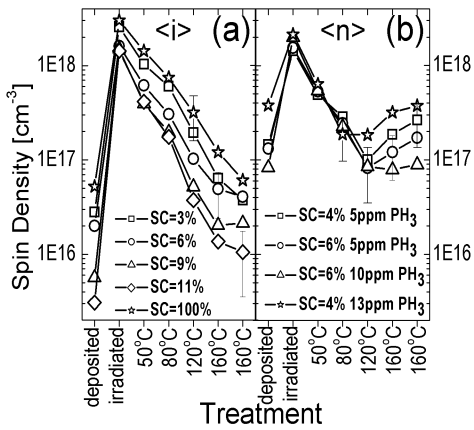


Fig. 3. Spin density of the intrinsic samples with different structure vs. treatment steps (a); Spin density of the PH₃-doped material vs. treatment steps (b)

In Fig. 4 (a&b) some of the spectra are shown for intrinsic $\mu\text{c-Si:H}$ and a-Si:H. As one can see the satellites being pronounced after irradiation are more sensitive to the annealing and already at 50 °C their relative contribution is clearly reduced. In the majority of cases spectra of annealed material return to the initial line shape.

In the Fig. 3,b N_s of n-doped samples are presented. One has to mention, that in the initial state the db resonance in the n-doped material is reduced or not detectable at all, but the conduction electron (CE) line arises with doping level increase [12], as shown on the Fig. 4,c (top line).

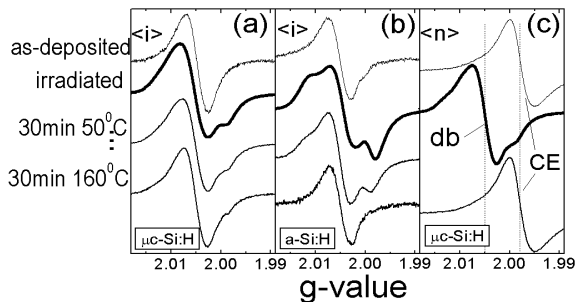


Fig. 4. Spectra after deposition, after irradiation and on two annealing points: a – intrinsic $\mu\text{c-Si:H}$; b – intrinsic a-Si:H; c – 10 ppm PH₃-doped $\mu\text{c-Si:H}$

The reduction of the db line is caused by the shift of the Fermi level towards the conduction band. In this situation the db states become doubly occupied and are not detectable any more in the ESR experiment. Instead tail states of the conduction band get populated. After irradiation the resonance of the n-doped sample is identical to the intrinsic samples i.e. only db line (with above mentioned satellites) was observed (Fig. 4,c bold line). During annealing the CE resonance re-appears and after annealing at 120 °C becomes dominant again in the spectrum. Therefore we can observe a minimum of N_s when the position of the Fermi level is already above the midgap but is still below the level where majority of the donor states are situated. After annealing the return of the lineshape and the spin density was observed for the n-doped samples as well as for the intrinsic ones.

DISCUSSION

The increase of the defect density in the middle of the gap in the same sample was the central idea of the irradiation experiment. One of the important requirements for this approach is maintenance of the material microstructure during the whole experiment. From the reversibility of the irradiation effect we can conclude that the structure of the samples was not significantly affected by the treatment. Another important issue is that the position of the created defects is within the bandgap of the material. The fact is supported with two observations: (i) the resonance of the intrinsic samples was not shifted after irradiation (ii) the observation of the db resonance in the n-doped samples indicates the Fermi level shift in the middle of the gap.

One should consider now the appearance of the new features in the resonance of irradiated samples (Fig. 2,a). This observation was not reported by other groups and was an unexpected outcome of the experiment. The structure of the features is different for $\mu\text{c-Si:H}$ and a-Si:H. For the a-Si:H samples prepared with different SC there is no significant difference in the structure of satellites but their relative contribution is different. The origin of the satellites is not identified at the moment therefore the line shape of these satellites could not be evaluated unambiguously. There are number of possible origins of the satellites: hyperfine interaction with hydrogen nuclei, creation of centres with high anisotropy which lead to a complex powder spectrum line, the spin-spin interaction in the local areas with high N_s , creation of the new defects in a special environment, and of course the combination of these reasons could not be excluded. The choice of the model will affect the estimation of the contribution of satellites. We have estimated the contribution of the satellites for the a-Si:H after irradiation assuming, for simplicity, the constancy of the central line shape. The simulation procedure is presented in Fig. 5.

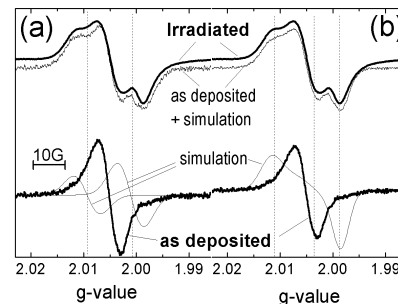


Fig. 5. The simulation of the satellites contribution with two approaches: contributions assumed to be Gaussian lines (a); additional spectrum assumed to be the powder pattern of the anisotropic state (b)

CONCLUSIONS

The first important outcome of the work is the successful application of MeV electron bombardment as a tool for reversible increase of the defect density in $\mu\text{-Si:H}$ and a-Si:H . The defects were created in the band gap of the material and likely have the same origin as defects before irradiation. The experiment being applied for the single layers of $\mu\text{-Si:H}$ and a-Si:H as well as to devices on their basis could result in new information on the role of defects in the electronic properties of the material.

New features were observed in the irradiated material appearing as satellites on the central (db) line. Their shape and contribution is dependent on the particular material structure. The origin of the satellites is currently not identified. The states responsible for the satellites are less stable at elevated temperatures than the db like defects thus the low temperature irradiation and sample storage is critical for the observation of the satellites. Possibly due to this reason no reports on the satellite appearance was found despite many irradiation experiments were done by other groups [15, 16].

REFERENCES

1. R. Schropp, M. Zeman. *Amorphous and microcrystalline silicon solar cells: modeling, materials and device technology*. Boston, Mass. Kluwer Academic Publ. 1998, ISBN 0-7923-8317-6.
2. R.A. Street. *Hydrogenated amorphous silicon*. Cambridge University Press, 1991.
3. R.A. Street, D.K. Biegelsen // *Topics in applied physics*. 1984, v. 56, p. 198–208.
4. C. Poole. *Electron spin resonance: a comprehensive treatise on experimental techniques*. New York: Wiley, 1983.
5. M. Stutzmann, D. Biegelsen // *Phys. Rev. B*. 1989, v. 40, p. 14.
6. J. Müller, F. Finger, R. Carius, H. Wagner // *Phys. Rev. B* 60. 1999, p. 16.
7. M.M. de Lima, P.C. Taylor, S. Morrison, A. LeGeune, F.C. Marques // *Phys. Rev. B* 65. 2002, p. 235324.
8. S. Yamasaki, T. Umeda, J. Isoya, J.H. Zhou, K. Tanaka // *J. Non-Cryst. Solids*. 1998, v. 227-230, p. 332–337.
9. O. Astakhov, F. Finger, R. Carius, A. Lambertz, Yu. Petrusenko, V. Borysenko, D. Barankov // *J. Non-Cryst. Sol.* 2006, v. 352, p. 1020–1023.
10. L. Houben, M. Luysberg, P. Hapke, R. Carius, F. Finger, H. Wagner // *Philos. Mag.* 1998, v. A 77, p. 1447.
11. F. Finger, A.L.B. Neto, R. Carius, T. Dylla, S. Klein // *Phys. Stat. Solidi C*. 2004, v. 1, p. 1248–1254.
12. T. Dylla, R. Carius, F. Finger // *Mat. Res. Soc. Symp. Proc.* 2002, v. 715, p. A20.9.1.
13. A.L. B. Neto, T. Dylla, S. Klein, T. Repmann, A. Lambertz, R. Carius, F. Finger // *J. Non-Cryst. Sol.* 2004, v. 338–340, p. 168–172.
14. J.W. Corbett. *Electron radiation damage in semiconductors and metals* New-York. NY: Academic Pr., 1966.
15. R. Street, D. Biegelsen, J. Stuke // *Philosophical Magazine B*. 1979, v. 40, N 6, p. 451–464.
16. W. Bronner, M. Mehring, R. Brüggemann // *Phys. Rev. B*. 2002, v. 65, p. 165212.

ПАРАМАГНИТНЫЕ ЦЕНТРЫ В АМОРФНОМ И МИКРОКРИСТАЛЛИЧЕСКОМ КРЕМНИИ, ОБЛУЧЕННОМ 2 МэВ ЭЛЕКТРОНАМИ

А. Астахов, Ф. Фингер, Р. Кариус, А. Ламбертз, И. Неклюдов, Ю. Петрусенко, В. Борисенко, Д. Баранков

Аморфный и микрокристаллический кремний являются широко известными материалами для производства тонкопленочной электроники большой площади. Дефекты в данных материалах играют решающую роль для качества приборов и оптимизации производственных процессов. Мы исследовали тонкопленочный гидрогенированный кремний методом измерений электронного парамагнитного резонанса (ЭПР). Для изменения плотности дефектов в широких пределах образцы облучались электронами с энергией 2 МэВ. Образцы исследовались после осаждения, после облучения и между стадиями отжига. Плотность спинов (N_s) в материале изменялась в пределах 3-х порядков величины. По обе стороны от центрального резонанса, характеризующего оборванные связи кремния, наблюдались мощные дополнительные резонансные линии ($g \approx 2.010$ и $g \approx 2.000$). После отжига форма резонансных линий и плотность спинов возвращались к исходным значениям.

ПАРАМАГНИТНІ ЦЕНТРИ У АМОРФНОМУ І МІКРОКРИСТАЛІЧНОМУ КРЕМНІІ, ОПРОМІНЕНОМУ 2 МеВ ЕЛЕКТРОНАМИ

О. Астахов, Ф. Фингер, Р. Кариус, А. Ламбертз, И. Неклюдов, Ю. Петрусенко, В. Борисенко, Д. Баранков

Аморфний і мікрокристалічний кремній є широко відомими матеріалами для виробництва тонкоплівкової електроніки великої площі. Дефекти у даних матеріалах відіграють вирішальну роль для якості пристроїв і оптимізації виробничих процесів. Ми досліджували тонкоплівковий гідрогенований кремній методом вимірів електронного парамагнітного резонансу (ЕПР). Для зміни щільності дефектів у широкому діапазоні зразки було опромінено електронами з енергією 2 МеВ. Зразки було досліджено після осадження, після опромінення і між етапами відпалу. Щільність спинів (N_s) в матеріалі змінювалась в межах 3-х порядків величини. З обох боків від центрального резонансу, що характеризує обірвані зв'язки кремнію, спостерігались потужні додаткові резонансні лінії ($g \approx 2.010$ і $g \approx 2.000$). Після відпалу форма резонансних ліній і щільність спинів поверталися до вихідних показників.